Table S1. Biomechanical Properties of Femur

	Male			Female		
	Control	*BT^{KO}*	p-value	Control	*BT^{KO}*	p-value
N	13	10		10	10	
Whole Bone Mechanical Properties						
Yield Load (N)	11.09 ± 0.617	7.853 ± 0.584	0.0013	9.880 ± 0.315	5.447 ± 0.711	< 0.0001
Stiffness	102.9 ± 5.35	83.23 ± 7.21	0.0357	62.77 ± 3.45	40.75 ± 4.41	0.0010
Tissue Level Biomechanics						
Yield Strain	0.016 ± 0.002	0.013 ± 0.001	0.3150	0.023 ± 0.001	0.018 ± 0.002	0.0972
Post Yield Strain	5.577 ± 0.762	0.392 ± 0.068	< 0.0001	6.425 ± 0.980	0.549 ± 0.154	< 0.0001
Total Strain	0.088 ± 0.006	0.027 ± 0.001	< 0.0001	0.096 ± 0.007	0.033 ± 0.004	< 0.0001
Young's Modulus (MPa)	6166 ± 423	4081 ± 327	0.0013	5178 ± 174	2566 ± 260	< 0.0001
Yield Stress (MPa)	76.36 ± 7.50	47.50 ± 5.60	0.0082	108.0 ± 7.86	42.18 ± 10.64	< 0.0001
Maximum Stress (MPa)	134.10 ± 5.90	70.91 ± 6.28	< 0.0001	160.10 ± 6.30	56.35 ± 6.70	< 0.0001
Failure Stress (MPa)	112.30 ± 7.00	51.88 ± 10.02	< 0.0001	151.00 ± 7.24	53.71 ± 7.50	< 0.0001
Toughness (MPa)	9.449 ± 0.865	1.196 ± 0.123	< 0.0001	12.40 ± 1.052	1.360 ± 0.248	< 0.0001
CSMOI (mm^4)	0.162 ± 0.008	0.195 ± 0.019	0.0937	0.101 ± 0.005	0.154 ± 0.005	< 0.0001

Values are recorded as mean ± SEM. N, number of animals; MPa, megapascals; CSMOI, cross sectional moment of inertia.

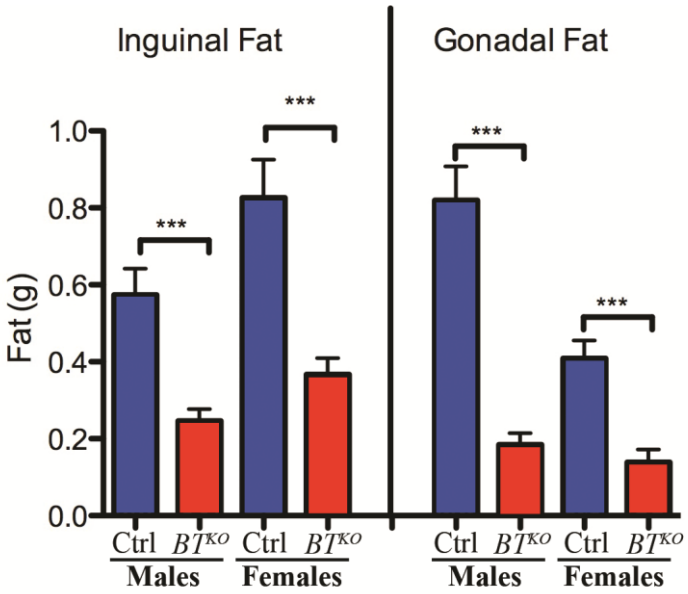

Figure S1. Reduction in weight of BT^{KO} adipose tissue. Inguinal and gonadal fat pads were dissected from control (Ctrl, blue) and BT^{KO} (red) mice, blotted, and weighed. Left and right fat pads were dissected from each mouse and the average weight used as the fat pad weight for that mouse. (n=10 for all groups except for BT^{KO} males, for which n=13).

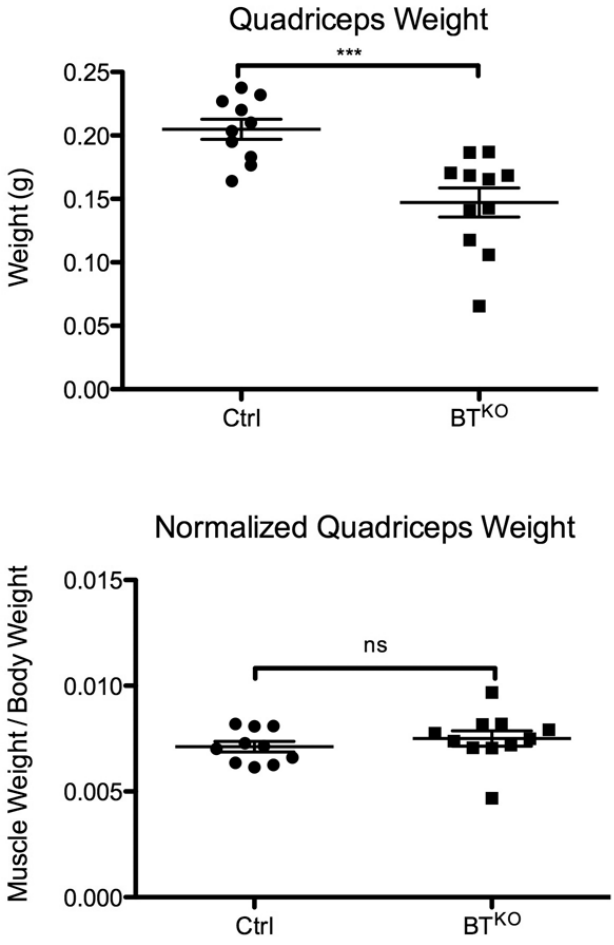

Figure S2. BT^{KO} muscle mass is reduced compared to that of controls, proportionate to reduced BT^{KO} body mass. As a representative example of the generalized reduced mass of BT^{KO} muscle, compared to controls, quadriceps were dissected out, blotted and weighed. Left and right quadriceps were dissected from male mice and the average weight used as the quadriceps weight for that mouse. Controls (Ctrl), n=10, and BT^{KO}, n=11. Bottom panel shows the reduction in mass of BT^{KO} quadriceps to be proportionate to the reduced mass of mice BT^{KO} mice themselves, by dividing the averaged weights of the quadriceps of each mouse by the weight of that mouse.

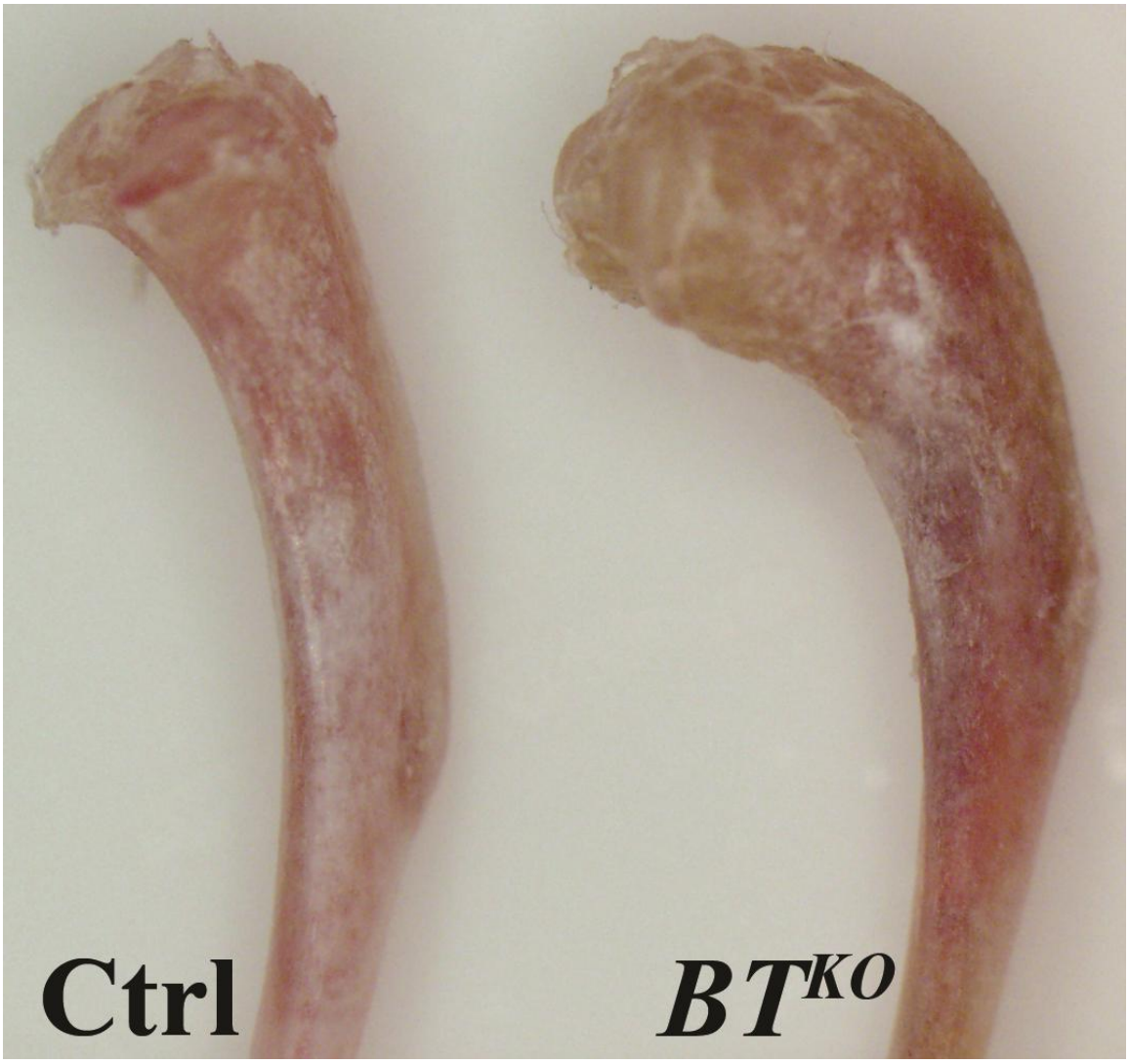

Figure S3. Some BT^{KO} mice showed flaring of proximal tibias. A photograph is shown of an example of flaring of the proximal tibia, seen in some BT^{KO} mice.

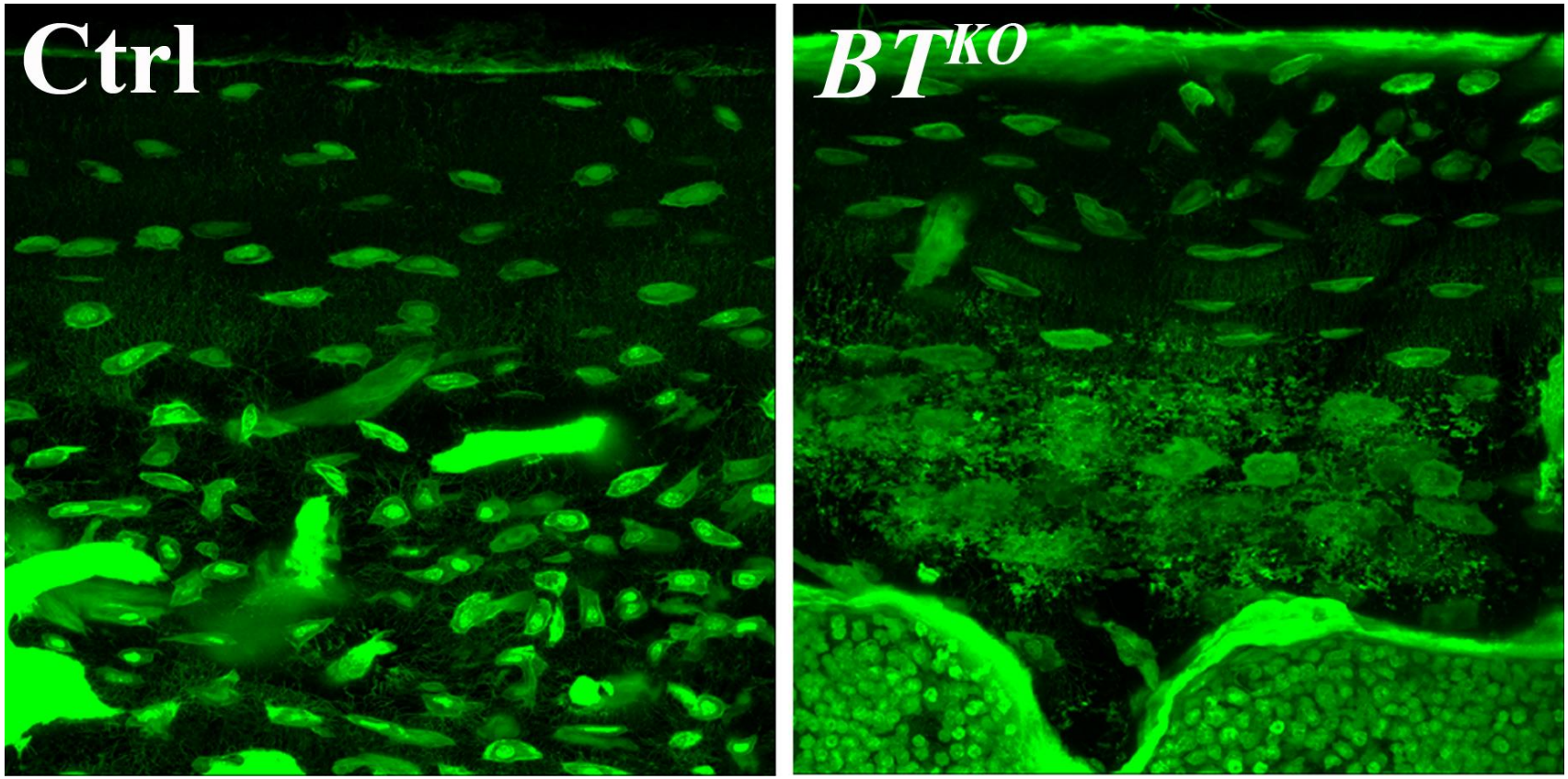

Figure S4. A portion of BT^{KO} osteocytes seemed unable to maintain the integrity of the lacunae in which they were located. A representative comparison is shown for FITC staining of cortical areas of femur, showing BT^{KO} osteocytes to have a loss of integrity of lacunae, resulting in increased penetration of FITC through lacunae walls (right panel), compared to controls (left panel).

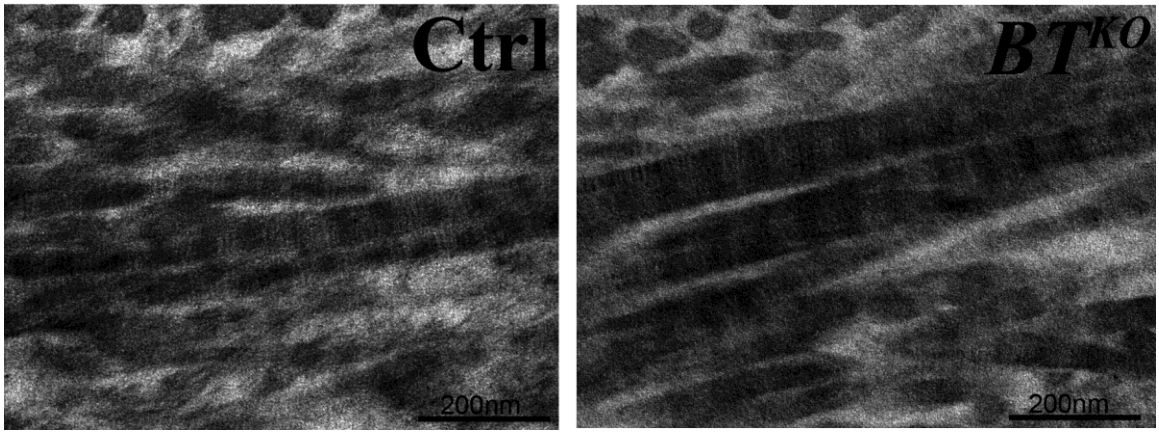

Figure S5. TEM comparison of BT^{KO} and control bone collagen fibrils. Unlike tendon collagen fibrils, bone collagen fibrils are not all parallel, and thus both longitudinal and cross-sections of collagen fibrils are seen in the same images for control (Ctrl) and BT^{KO} electron-micrographs.